2005 American Control Conference
June 8-10, 2005. Portland, OR, USA

Construction of Stochastic PDEs for Feedback Control of Surface Roughness in Thin Film Deposition

Dong Ni and Panagiotis D. Christofides
Department of Chemical Engineering
University of California, Los Angeles, CA 90095-1592

Abstract— **In this work, we develop a systematic method for the construction of linear stochastic partial differential equation (PDE) models for feedback control of surface roughness in thin film deposition. The method is applied to a representative deposition process and is successfully validated through simulations.**

I. INTRODUCTION

With the advancement of thin film technology, thin films of advanced materials are used in a very wide range of applications, e.g., microelectronic devices, optics, micro-electro-mechanical systems (MEMS) and biomedical products. Various deposition methods have been developed and widely used to prepare thin films such as physical vapor deposition (PVD) and chemical vapor deposition (CVD). However, the dependence of the thin film properties, such as uniformity, composition and microstructure, on the deposition conditions is a severe constraint on reproducing thin film's performance. Thus, real-time feedback control of thin film deposition becomes increasingly important in order to meet the stringent requirements on the quality of thin films and reduce thin film variability.

Earlier research efforts focus on feedback control of thin film deposition processes with emphasis on deposition spatial uniformity control (see [25], [4] for results on rapid thermal processing (RTP) and [1] on plasma-enhanced chemical vapor deposition (PECVD)) and on thin film composition control (see [21] for experimental results on real-time carbon content control in a PECVD process). More recently, motivated by the growing industrial demands, there have been significant research efforts focusing on modelling and control of thin film growth in order to obtain thin films with well-defined microstructure.

In a thin film growth process, the film is directly formed from microscopic random processes (e.g., molecule adsorption, desorption, migration and surface reaction). Precise control of film properties requires models that describe these microscopic processes and directly account for their stochastic nature. Examples of such models include: 1) kinetic Monte-Carlo (kMC) methods [9], [6], [10], and 2) stochastic partial differential equations (PDEs) [5], [28].

Kinetic Monte-Carlo methods can be readily developed and can describe the microscopic growth processes to atomistic details with multiple species and both short-range and long-range interactions. Methodologies for estimation-based control and model-predictive control using kinetic Monte-Carlo models have recently been developed in [12], [13] and [19], respectively. Furthermore, feedback control using kMC models has been successfully applied to control surface roughness in a $GaAs$ deposition process using experimentally determined model parameters [14]. Since kinetic Monte-Carlo simulations provide realizations of a stochastic process which are consistent with the master equation which describes the evolution of the microscopic probability distribution, a method to construct reduced-order approximations of the master equation was also reported in [7].

However, the fact that kMC models are not available in closed-form makes very difficult to use them for system-level analysis and the design and implementation of real-time model-based feedback control systems. Motivated by this, an approach was reported in [23], [2] to identify linear deterministic models from outputs of kinetic Monte-Carlo simulators and design controllers using linear control theory to control the macroscopic variables which are low statistical moments of the microscopic distributions (e.g., surface coverage, which is the zeroth moment of adspecies distribution on a lattice). However, to control higher statistical moments of the microscopic distributions, such as the surface roughness (the second moment of height distribution on a lattice), or even the microscopic configuration (such as the surface morphology), linear deterministic models may not be sufficient, because the effect of the stochastic nature of the microscopic processes becomes very significant and must be addressed both in the model construction and controller design.

Stochastic PDE models, on the other hand, which are available in closed-form, have been developed to describe the evolution of the height profile for surfaces in certain physical and chemical processes such as epitaxial growth [28] and ion sputtering [11]. More recently, Lou and Christofides [16] presented a method for feedback control of surface roughness in a thin film growth process whose surface height fluctuation can be described by the Edwards-Wilkinson equation [5], a second-order stochastic

0-7803-9098-9/05/$25.00 ©2005 AACC

parabolic PDE (see also [15] for results on control of surface roughness in a sputtering process using the stochastic Kuramoto-Sivashinsky equation). A feedback controller was designed based on the stochastic PDE model and successfully applied to the kMC model of the deposition process regulating the surface roughness to desired values. However, the construction of stochastic PDE models for thin film growth processes directly based on microscopic process rules [17], [22], [27] is a very difficult task. This issue has prohibited the development of stochastic PDE models, and subsequently the design of model-based feedback control systems, for realistic deposition processes which are, in general, highly complex.

In this work, we develop a systematic method for the construction of linear stochastic PDE models for feedback control of surface roughness in thin film deposition. A linear stochastic PDE model is constructed for a generic thin film deposition process and is used to design a real-time feedback controller to control the thin film surface roughness. We initially reformulate a general linear stochastic PDE into a system of infinite stochastic ordinary differential equations (ODE) by using modal decomposition and derive the analytical expressions of the first and second statistical moments of the ODE states. Then, we use a kMC code to generate surface snapshots for different instants during process evolution to obtain values of the state vector of the stochastic ODE system. Subsequently, the eigenvalues and the covariances of the stochastic ODE system that correspond to the deposition process are computed based on the kMC simulation results. Finally, a linear stochastic PDE model is determined by least-square fitting the prederivative coefficients to match the spectrum of the stochastic PDE system to the identified spectrum of the stochastic ODE system. The dependence of the model parameters of the stochastic PDE on the process parameters is investigated and the least-square-optimal form of the stochastic PDE model with model parameters expressed as functions of the process parameters is determined. Furthermore, an optimization-based feedback controller is designed using the constructed stochastic PDE model and applied to the kMC simulation of the deposition process to control the surface roughness. Closed-loop system simulation results demonstrate that the model is adequately accurate and that the controller is capable of controlling the surface roughness of the thin film.

II. PRELIMINARIES

In this work, we consider a thin film growth process of deposition from vapor phase on a 1-dimensional lattice, in which, the formation of the thin film is governed by two microscopic processes that occur on the surface as shown in Fig.1, i.e., the adsorption of vapor phase molecules on the surface and the migration of surface molecules (see [20] for the extension of this work to a 2-dimensional growth process with molecule desorption). This process is, in fact, a very common thin film growth process that can be traced in most chemical vapor deposition processes. A kinetic Monte-Carlo simulation code following the algorithm reported in [26] is used to simulate the deposition process and obtain surface snapshots.

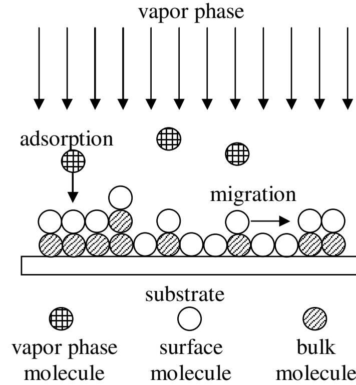

Fig. 1. The thin film growth process.

As we discussed in the introduction, although there exist many first principles-based simulation codes for simulating the microscopic processes, most of them are computationally very expensive. Therefore, closed-form stochastic PDE models are favored for applications in which computation efficiency is essential, such as, for the purpose of model-based real-time feedback control.

Without any *a priori* knowledge of the deposition process, we assume that there exists a one-dimensional linear stochastic PDE of the following general form that can adequately describe the evolution of the surface of the thin film during the deposition:

$$\frac{\partial h}{\partial t} = c + c_0 h + c_1 \frac{\partial h}{\partial x} + c_2 \frac{\partial^2 h}{\partial x^2} + \cdots + c_w \frac{\partial^w h}{\partial x^w} + \xi(x,t) \quad (1)$$

where $x \in [0, \pi]$ is the spatial coordinate, t is the time, $h(x,t)$ is the height of the surface at position x and time t, and $\xi(x,t)$ is a Gaussian noise with zero mean and covariance:

$$\langle \xi(x,t)\xi(x',t') \rangle = \varsigma^2 \delta(x-x')\delta(t-t') \quad (2)$$

where $\delta(\cdot)$ is the Dirac function. Furthermore, the prederivative coefficients c and c_j in Eq.1 and the parameter ς^2 in Eq.2 depend on the process parameters (gas flow rates, substrate temperature, etc.) $p_i(t)$:

$$\begin{aligned} c &= C[p_1(t), p_2(t), \cdots, p_d(t)] \\ c_j &= C_j[p_1(t), p_2(t), \cdots, p_d(t)] \quad j = 0, \cdots, w \\ \varsigma^2 &= C_\xi[p_1(t), p_2(t), \cdots, p_d(t)] \end{aligned} \quad (3)$$

where $C(\cdot)$, $C_j(\cdot)$ and $C_\xi(\cdot)$ are nonlinear functions to be determined.

The stochastic PDE of Eq.1 is subjected to the following periodic boundary conditions:

$$\frac{\partial^j h}{\partial x^j}(0,t) = \frac{\partial^j h}{\partial x^j}(\pi,t) \quad j = 0, \cdots, w-1 \quad (4)$$

and the initial condition:

$$h(x,0) = h_0(x) \quad (5)$$

To study the dynamics of Eq.1, we initially consider the eigenvalue problem of the linear operator of Eq.1, which takes the form:

$$\begin{aligned} A\phi_n(x) &= c_0\phi_n(x) + c_1\frac{d\phi_n(x)}{dx} + c_2\frac{d^2\phi_n(x)}{dx^2} + \cdots \\ &+ c_w\frac{d^w\phi_n(x)}{dx^w} = \lambda_n\phi_n(x) \\ \frac{d^j\phi_n}{dx^j}(0) &= \frac{d^j\phi_n}{dx^j}(\pi) \quad j = 0, \cdots, w-1; \quad n = 1, \cdots, \infty \end{aligned} \tag{6}$$

where λ_n denotes an eigenvalue and ϕ_n denotes an eigenfunction. A direct computation of the solution of the above eigenvalue problem yields:

$$\begin{aligned} \lambda_n &= c_0 + I2nc_1 + (I2n)^2c_2 + \cdots + (I2n)^w c_w \\ \phi_n(x) &= \sqrt{\frac{1}{\pi}}e^{I2nx} \quad n = 0, \pm 1, \cdots, \pm\infty \end{aligned} \tag{7}$$

where λ_n denotes the nth eigenvalue, $\phi_n(x)$ denotes the nth eigenfunction and $I = \sqrt{-1}$.

To present the method that we use for parameter identification of the stochastic PDE of Eq.1, we first derive an infinite stochastic ODE representation of Eq.1 using modal decomposition and parameterize the infinite stochastic ODE system using kMC simulation. We first expand the solution of Eq.1 in an infinite series in terms of the eigenfunctions of the operator of Eq.6 as follows (i.e., the Fourier expansion in the complex form):

$$h(x,t) = \sum_{n=-\infty}^{\infty} z_n(t)\phi_n(x) \tag{8}$$

where $z_n(t)$ are time-varying coefficients. Substituting the above expansion for the solution, $h(x,t)$, into Eq.1 and taking the inner product, the following system of infinite stochastic ODEs is obtained:

$$\frac{dz_n}{dt} = \lambda_n z_n + c_{zn} + \xi_n(t) \quad n = 0, \pm 1, \cdots, \pm\infty \tag{9}$$

and the initial conditions:

$$z_n(0) = z_{n0} \quad n = 0, \pm 1, \ldots, \pm\infty \tag{10}$$

where $c_{zn} = c\int_0^\pi \phi_n(x)dx$ (apparently $c_{z0} = c\sqrt{\pi}$ and $c_{zn} = 0 \ \forall \ n \neq 0$), $\xi_n(t) = \int_0^\pi \xi(x,t)\phi_n(x)dx$ and $z_{n0} = \int_0^\pi h_0(x)\phi_n(x)dx$.

The covariances of $\xi_n(t)$ can be computed by using the following result:

Result 1: If (1) $f(x)$ is a deterministic function, (2) $\eta(x)$ is a random variable with $\langle\eta(x)\rangle = 0$ and covariance $\langle\eta(x)\eta(x')\rangle = \sigma^2\delta(x-x')$, and (3) $\epsilon = \int_a^b f(x)\eta(x)dx$, then ϵ is a random number with $\langle\epsilon\rangle = 0$ and covariance $\langle\epsilon^2\rangle = \sigma^2\int_a^b f^*(x)f(x)dx$ [3].

Using Result 1, we obtain $\langle\xi_n(t)\rangle = 0$ and $\langle\xi_n(t)\xi_n^*(t')\rangle = \varsigma^2\delta(t-t')$ (ξ_n^* is the complex conjugate of ξ_n, the superscript star is used to denote complex conjugate in the remainder of this manuscript). We note that $\xi_n(t)$ is a complex Gaussian random variable and the probability distribution function of the Gaussian distribution, $P(\xi_n,t)$, on the complex plane with zero mean and covariance $\varsigma^2\delta(t-t')$ is defined as follows:

$$P(\xi_n,t) = \frac{1}{\sqrt{2\pi}\varsigma\delta(t-t')}e^{\dfrac{\xi_n\xi_n^*}{2\varsigma^2\delta(t-t')}} \tag{11}$$

To parameterize this system of infinite stochastic ODEs, we first derive the analytic expressions for the statistical moments of the stochastic ODE states, including the expected value and covariance. By comparing the analytical expression to the statistical moments obtained by multiple kMC simulations, the parameters of the stochastic ODE system (i.e., λ_n and ς) can be determined.

The analytic solution of Eq.9 is obtained as follows to derive the expressions for the statistical moments of the stochastic ODE states:

$$z_n(t) = e^{\lambda_n t}z_{n0} + \frac{(e^{\lambda_n t}-1)c_{zn}}{\lambda_n} + \int_0^t e^{\lambda_n(t-\mu)}\xi_n(\mu)d\mu \tag{12}$$

Using Result 1, Eq.12 can be further simplified as follows:

$$z_n(t) = e^{\lambda_n t}z_{n0} + \frac{(e^{\lambda_n t}-1)c_{zn}}{\lambda_n} + \theta_n(t) \tag{13}$$

where $\theta_n(t)$ is a complex random variable of normal distribution with zero mean and covariance $\langle\theta_n(t)\theta_n^*(t)\rangle = \varsigma^2\dfrac{e^{(\lambda_n+\lambda_n^*)t}-1}{\lambda_n+\lambda_n^*}$. Therefore, the expected value (the first stochastic moment) and the covariance (the second stochastic moment) of state z_n can be expressed as follows:

$$\begin{aligned} \langle z_n(t)\rangle &= e^{\lambda_n t}z_{n0} + \frac{(e^{\lambda_n t}-1)c_{zn}}{\lambda_n} \\ \langle z_n(t)z_n^*(t)\rangle &= \varsigma^2\frac{e^{(\lambda_n+\lambda_n^*)t}-1}{\lambda_n+\lambda_n^*} + \langle z_n(t)\rangle\langle z_n(t)\rangle^* \\ n &= 0, \pm 1, \cdots, \pm\infty \end{aligned} \tag{14}$$

Eq.14 holds for any initial condition z_{n0}. Since we are able to choose any initial thin film surface for simulation, we choose $z_{n0} = 0$ (i.e., the initial surface is flat, $h(x,0) = 0$) to simplify our calculations. In this case, Eq.14 can be further simplified as follows (note that $c_{zn} = 0, \forall n \neq 0$):

$$\begin{aligned} \langle z_n(t)\rangle &= 0 \\ \langle z_n(t)z_n^*(t)\rangle &= \varsigma^2\frac{e^{(\lambda_n+\lambda_n^*)t}-1}{\lambda_n+\lambda_n^*} = \varsigma^2\frac{e^{2Re(\lambda_n)t}-1}{2Re(\lambda_n)} \\ n &= \pm 1, \cdots, \pm\infty \end{aligned} \tag{15}$$

where $Re(\lambda_n)$ denote the real part of λ_n, and for $z_0(t)$, it

follows from Eq.14 with $\lambda_0 = 0$ that

$$\langle z_0(t)\rangle = \lim_{\lambda_0\to 0} \frac{(e^{\lambda_0 t} - 1)c_{z0}}{\lambda_0} = tc_{z0} = t\sqrt{\pi}c$$
$$\langle z_0^2(t)\rangle = \varsigma^2 t + t^2\pi c^2 \tag{16}$$

It can be seen in Eq.15 that the statistical moments of each stochastic ODE state depend only on the real part of the corresponding eigenvalue, and therefore, to determine the imaginary part of the eigenvalue we construct an extra equation related to the expected value of $Re[\lambda_n(t)]^2$ (not shown here due to space limitations). We note that λ_n would be a complex number if the linear operator A is not self-adjoint when odd-partial-derivatives are present in the stochastic PDE (see Eq.7).

III. Model construction

Based on the results shown in the previous section, we propose a systematic procedure to construct a linear stochastic PDE for the deposition process described in Section 2.1. This procedure can be readily extended to other stochastic processes. In this work, we use a kinetic Monte-Carlo code to simulate the deposition process and generate surface snapshots.

The proposed procedure includes the following steps: First, we design a set of simulation experiments that cover the complete range of process operation; second, we run multiple simulations for each simulation experiment to obtain the trajectories of the first and second statistical moments of the states (i.e., Fourier coefficients) computed from the surface snapshots; third, we compute the eigenvalues of the linear operator and covariance of the Gaussian noise based on the trajectories of the statistical moments of the states for each simulation experiment, and determine the model parameters of the stochastic PDE (i.e., the pre-derivative coefficients and the order of the stochastic PDE); finally, we investigate the dependence of the model parameters of the stochastic PDE on the process parameters and determine the least-square-optimal form of the stochastic PDE model with model parameters expressed as functions of the process parameters.

A. Eigenvalues and covariance

Because there are only two process parameters considered in the deposition process studied in this work, the growth rate W and the substrate temperature T, the simulation experiment design is straightforward. Specifically, different W values and T values are evenly selected from the range of process operation of interest and simulation experiments are executed with every selected W value for each selected T value. Therefore, we start our demonstration of the model construction methodology with the identification of the eigenvalues and covariance. Also, we note that the trajectories of the statistical moments for each simulation experiment are computed based on 100 simulation runs taking place with the same process parameters.

In the previous section we have shown that for a deposition process with a flat initial surface, the covariance of each state $\langle z_n(t)z_n^*(t)\rangle$ should be able to be predicted by Eq.15, therefore, we can fit ς^2 and $Re(\lambda_n)$ in Eq.15 for the profile of $\langle z_n(t)z_n^*(t)\rangle$.

In order to obtain the profile of $\langle z_n(t)z_n^*(t)\rangle$, we need to generate snapshots of the thin film surface during each deposition simulation and compute the values of $z_n(t)$. Since the lattice consists of discrete sites, we let $h(kL,t)$ be the height profile of the surface at time t with lattice constant L (k denotes the coordinate of a specific surface site), and compute $z_n(t)$ as follows:

$$\begin{aligned} z_n(t) &= \int_0^{\pi} h(x,t)\phi_n^*(x)dx \\ &= \sum_{k=0}^{k_{max}} h(kL,t)\int_{kL}^{(k+1)L} \phi_n^*(x)dx \end{aligned} \tag{17}$$

where $k_{max}L = \pi$ (i.e., the lattice is mapped to the domain [0,π]). Substituting Eq.7 into Eq.17, we can derive the following expression for $z_n(t)$:

$$\begin{aligned} z_n(t) &= \sum_{k=0}^{k_{max}} \frac{h(kL,t)e^{-2kLnI}}{2\sqrt{\pi}nI}(1 - e^{-2LnI}) \\ n &= \pm 1, \cdots, \pm\infty \end{aligned} \tag{18}$$

and for $z_0(t)$, we have,

$$z_0(t) = \sum_{k=0}^{k_{max}} h(kL,t)\frac{L}{\sqrt{\pi}} = \sqrt{\pi}t\frac{\sum_{k=0}^{k_{max}} h(kL,t)}{k_{max}t} = t\sqrt{\pi}W \tag{19}$$

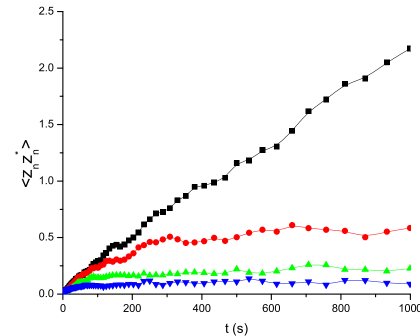

Fig. 2. Covariance profiles of z_{10}, z_{20}, z_{30} and z_{40}.

To capture the dynamics of both the fast states and slow states simultaneously in the same simulation run with few surface snapshots, the snapshots are generated in a variable-time-step fashion in which the intervals between two snapshots are increased with time. This procedure is motivated by the fact that the dynamics of the fast states can be detected only at the beginning of each simulation run, and therefore, the evolving surface should be sampled more frequently in the beginning than the remainder to cope with the small time scale of these fast states.

Fig.2 shows the typical covariance profiles of different states in a growth process. It can be seen that despite the

very different time scales of the states, our method can still generate very smooth profiles for both the fast states (such as z_{40}, whose time scale is less than 50 s) and the slow states (such as z_{10}, whose time scale is larger than 1000 s).

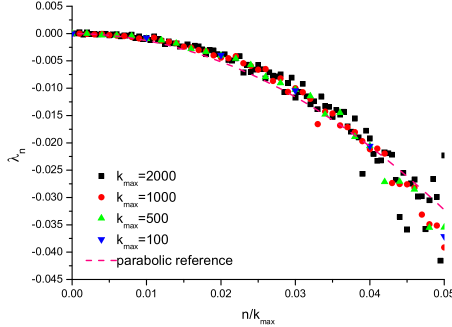

Fig. 3. Eigenvalue spectrums of the infinite stochastic ODE systems identified from the kMC simulation of the deposition process with different lattice size: $k_{max} = 100$, $k_{max} = 500$, $k_{max} = 1000$ and $k_{max} = 2000$.

Fig.3 shows the eigenvalues identified from thin film depositions occurring under the same operating conditions but simulated with different lattice size (we note that the identified eigenvalues are considered real since the imaginary part of the eigenvalues identified turned out to be very small). It can be seen that the identified spectrums are very close to each other when n is rescaled with the corresponding lattice size. This is expected, since, $\phi_n(x)$ is a basis of the domain of operator A, and is a complex function of the frequency n. Accordingly, n/k_{max} is the length scale of the surface fluctuation described by $\phi_n(x)$ when a lattice of size k_{max} is mapped to the domain of $[0, \pi]$ (we note that, for the same reason, the covariance values should be scaled with the inverse of the lattice size, $1/k_{max}$, in order to carry out a meaningful comparison).

It can also be seen in Fig.3 that the eigenspectrums are very close to the parabolic reference curve, which implies that a second-order stochastic PDE system of the following form would be able to describe the evolution of the surface height of this deposition process:

$$\frac{\partial h}{\partial t} = c + c_2 \frac{\partial^2 h}{\partial x^2} + \xi(x,t) \quad (20)$$

in which c, c_2 and the covariance of the Gaussian noise ξ, ς, all depend on the microscopic processes and operating conditions.

B. Dependence on the process parameters

We proceed now with the derivation of the parameters of the stochastic PDE of Eq.20. From Eq.16 and Eq.19, we can see that $c = W$ for all cases. However, c_2 and ς^2 identified for different deposition settings can be very different, therefore, we need to investigate their dependence on the deposition parameters to obtain their analytical expressions. c_2 and ς^2 are evaluated for assorted deposition conditions and a lattice size of 1000 (i.e., $k_{max} = 1000$) is used for all the simulation runs in our study.

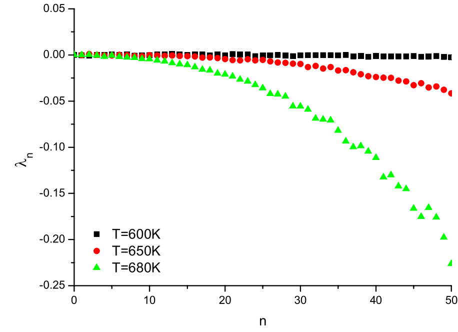

Fig. 4. Eigenvalue spectrums identified from simulated deposition processes with a growth rate $W = 0.5ML/s$ for different substrate temperatures: $T = 600K$, $T = 650K$ and $T = 680K$.

Fig.4 shows the eigenspectrums identified from depositions with the same growth rate ($W = 0.5\ monolayer \cdot s^{-1}$) for different substrate temperatures. It can be seen that the magnitude of the eigenvalues decreases faster with increasing n at higher substrate temperature. This implies that a higher substrate temperature corresponds to a larger c_2 in the stochastic PDE model and vice versa.

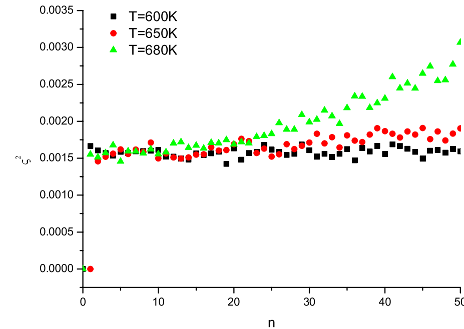

Fig. 5. Covariance spectrums identified from simulated deposition processes with a growth rate $W = 0.5ML/s$ for different substrate temperatures: $T = 600K$, $T = 650K$ and $T = 680K$.

Fig.5 shows the covariance spectrums identified from depositions with the same growth rate ($W = 0.5\ monolayer \cdot s^{-1}$) for different substrate temperature. Although it follows from Eq.11 that the covariance of the stochastic noise should be the same for all states, it is not so for high-order states in the high substrate temperature regime (e.g., $T = 680\ K$). However, because these high order states correspond to the surface fluctuations of small length scales, and at the same time, such small length scale surface fluctuations are almost negligible in the high substrate temperature regime due to the significant surface diffusion, the contribution from these high-order states at high substrate temperature becomes very small. Therefore, given that such discrepancy would not significantly affect the accuracy of the model, we compute ς^2 only based on the low-order states. From the covariance of the low-order states shown in Fig.5, we may also consider ς^2 to be independent of substrate temperature.

Fig.6 shows the eigenspectrums identified from deposi-

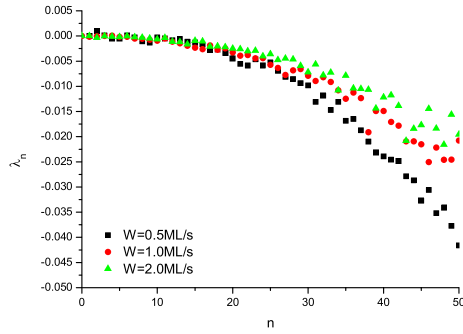

Fig. 6. Eigenvalue spectrums identified from simulated deposition processes with a substrate temperature $T = 650K$ for different growth rates: $W = 0.5ML/s$, $W = 1.0ML/s$ and $W = 2.0ML/s$.

tions occurring under the same substrate temperature ($T = 650K$) and different thin film growth rates. It can be seen that, at this substrate temperature, the eigenvalues die out a bit slower with increasing growth rate, which implies that a higher growth rate corresponds to a smaller c_2 in the stochastic PDE model and vice versa.

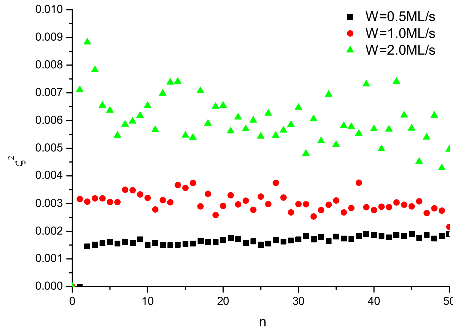

Fig. 7. Covariance spectrums identified from simulated deposition processes with a substrate temperature $T = 650K$ for different growth rates: $W = 0.5ML/s$, $W = 1.0ML/s$ and $W = 2.0ML/s$.

Fig.7 shows the covariance spectrums identified from depositions occurring under the same substrate temperature ($T = 650K$) and different thin film growth rates. It can be seen that a higher growth rate corresponds to a larger covariance value.

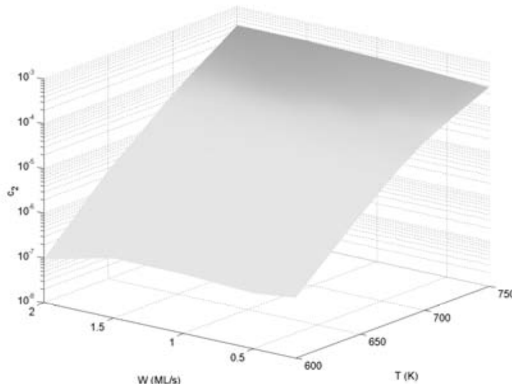

Fig. 8. Profile of c_2 as a function of substrate temperature T and thin film growth rate W.

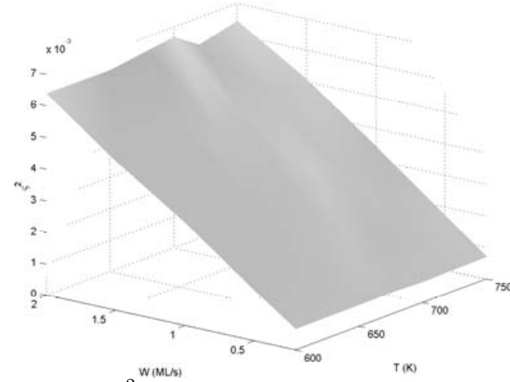

Fig. 9. Profile of ς^2 as a function of substrate temperature T and thin film growth rate W.

To derive explicit expressions for c_2 and ς^2 as functions of T and W, we evaluate these values for different T and W and the results are shown in Fig.8 and Fig.9. From Fig.8, we can see that $ln\, c_2$ has a quasi-linear relationship with both T and W, and thus, the following expression can be obtained for c_2 as a function of T and W through least square fitting:

$$c_2(T,W) = e^{-45.8176 + 0.0511T - 0.1620W} = \frac{e^{-32.002 + 0.0511T - 0.1620W}}{k_{max}^2} \quad (21)$$

From Fig.9 we can see that ς^2 depends almost linearly on both T and W, and thus, the following expression can be obtained for ς^2 as a function of T and W through least square fitting as well:

$$\varsigma^2(T,W) = 5.137 \times 10^{-8}T + 3.2003 \times 10^{-3}W \approx \frac{\pi W}{k_{max}} \quad (22)$$

Therefore, the linear stochastic PDE model identified for the deposition process is as follows:

$$\frac{\partial h}{\partial t} = W + (\frac{e^{-32.002 + 0.0511T - 0.1620W}}{k_{max}^2})\frac{\partial^2 h}{\partial x^2} + \xi(x,t); \ \frac{\partial h}{\partial x}(0,t) = \frac{\partial h}{\partial x}(\pi,t), \ h(0,t) = h(\pi,t) \quad (23)$$

where $\langle \xi(x,t)\xi(x',t')\rangle = (5.137 \times 10^{-8}T + 3.2003 \times 10^{-3}W)\delta(x-x')\delta(t-t')$.

C. Validation of stochastic PDE model

We now proceed with the validation of the stochastic PDE model of the thin film deposition process (Eq.23). Validation experiments are conducted for a number of deposition conditions which have not been used for the model construction. We generate surface profiles using both the stochastic PDE model and the kinetic Monte-Carlo code. Fig.10 shows the surface profile at the end of a deposition with substrate temperature $T = 550\ K$, thin film growth rate $W = 0.1\ monolayer \cdot s^{-1}$, deposition duration of $1000\ s$ and lattice size $k_{max} = 2000$; Fig.11 shows the surface profile at the end of a deposition with substrate

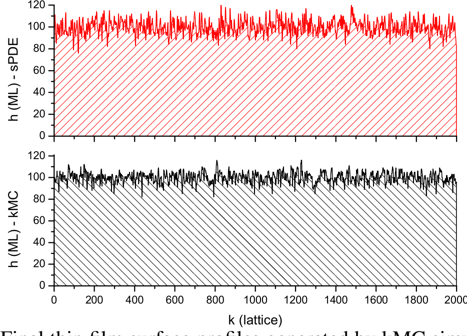

Fig. 10. Final thin film surface profiles generated by kMC simulation and stochastic PDE model for a $1000s$ deposition with substrate temperature $T = 550K$, thin film growth rate $W = 0.1\ monolayer \cdot s^{-1}$ and lattice size $k_{max} = 2000$.

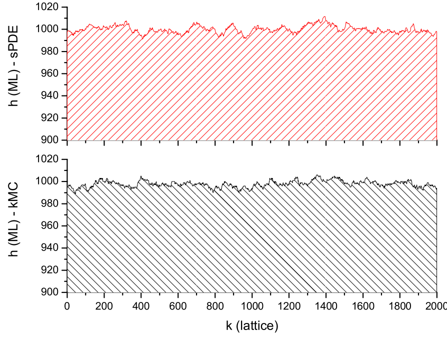

Fig. 11. Final thin film surface profiles generated by kMC simulation and stochastic PDE model for a $400s$ deposition with substrate temperature $T = 700K$, thin film growth rate $W = 2.5\ monolayer \cdot s^{-1}$ and lattice size $k_{max} = 2000$.

temperature $T = 700\ K$, thin film growth rate $W = 2.5$ $monolayer \cdot s^{-1}$, deposition duration of 400 s and lattice size $k_{max} = 2000$; we can see that both at low and high substrate temperatures, and for different growth rates, the linear stochastic PDE model constructed for the deposition process is very consistent with the kinetic Monte-Carlo simulation.

We also generate expected surface roughness profiles using both the stochastic PDE model and the kinetic Monte-Carlo simulation (average of 100 runs) for the deposition process. For simplicity, the surface roughness is evaluated in a root-mean-square fashion as follows:

$$r(t) = \sqrt{\frac{1}{\pi}\int_0^{\pi}[h(x,t) - \bar{h}(t)]^2 dx} \tag{24}$$

where $\bar{h}(t) = \dfrac{1}{\pi}\displaystyle\int_0^{\pi} h(x,t)dx$ is the average surface height. We note that for more detailed description of the surface morphology, the height-height correlation function may be used to evaluate the surface roughness [24].

Fig.12 shows the expected roughness profile of a deposition with substrate temperature $T = 550\ K$ and thin film growth rate $W = 0.1\ monolayer \cdot s^{-1}$; Fig.13 shows the roughness profile of a deposition with substrate temperature $T = 700\ K$ and thin film growth rate $W = 2.5$ $monolayer \cdot s^{-1}$; we can see that the linear stochastic PDE model constructed for the deposition process is also

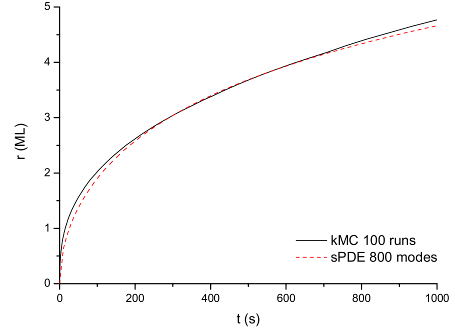

Fig. 12. Expected surface roughness profiles generated by kMC simulation and stochastic PDE model for a $1000s$ deposition with substrate temperature $T = 550K$, thin film growth rate $W = 0.1\ monolayer \cdot s^{-1}$ and lattice size $k_{max} = 2000$.

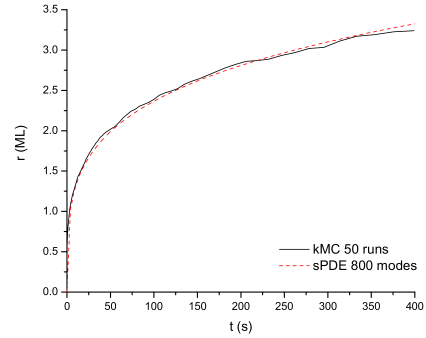

Fig. 13. Expected surface roughness profiles generated by kMC simulation and stochastic PDE model for a $400s$ deposition with substrate temperature $T = 700K$, thin film growth rate $W = 2.5\ monolayer \cdot s^{-1}$ and lattice size $k_{max} = 2000$.

very consistent with the kinetic Monte-Carlo simulation in terms of surface roughness, at both low and high substrate temperatures, for different growth rates.

IV. Feedback control

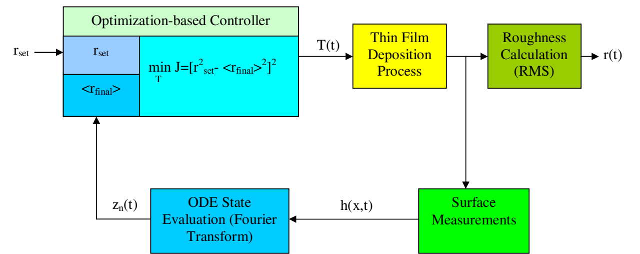

Fig. 14. Block diagram of the closed-loop system.

We now proceed with the design of the feedback controller. Since the thin film deposition is a batch process, the control objective is to control the final surface roughness of the thin film to a desired level at the end of each deposition run. Therefore, we use an optimization-based control problem formulation. Fig.14 shows the block diagram of the closed-loop system. When a real-time surface profile measurement is obtained, the states of the infinite stochastic ODE system, z_n, are computed. Then, a substrate

temperature T is computed based on states z_n and the stochastic PDE model and applied to the deposition process. The substrate is held at this temperature for the rest of the deposition until a different value is assigned by the controller. The value of T is determined at each time t by solving, in real-time, an optimization problem minimizing the difference between the estimated final surface roughness and the desired level. A standard procedure based on the active set method [8] is used to solve the optimization problem. A kMC code with a lattice size $k_{max} = 1000$ is used to simulate the thin film deposition process, and the substrate temperature is restricted within 300 K to 900 K. The measurement interval, as well as the control interval, is set to be 1 s. We limit the maximum number of states to be used (in our case, to $m = 500$) to guarantee the maximum possible computation time for each control action is within certain requirement, however, for most of the time the number of states needed by the controller is much smaller.

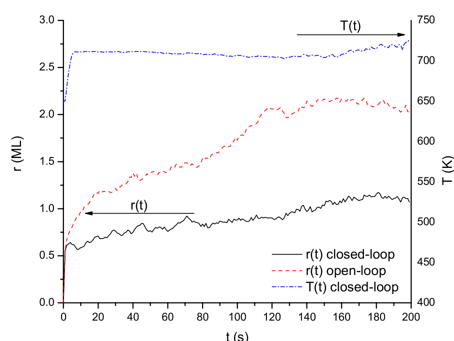

Fig. 15. Surface roughness and substrate temperature profiles of a 1000 s closed-loop deposition process with thin film growth rate $W = 0.5$ $monolayer \cdot s^{-1}$ and final roughness setpoint $r_{set} = 1.0$ $monolayer$.

Fig.15 shows the surface roughness and substrate temperature profiles of a closed-loop deposition process with thin film growth rate $W = 0.5$ $monolayer \cdot s^{-1}$. The control objective is to drive the final surface roughness of the thin film to 1.0 $monolayer$ at the end of the 1000 s deposition. It can be seen that the final surface roughness is controlled at the desired level while an open-loop deposition with the same initial deposition condition would lead to a 100% higher final surface roughness as shown in Fig.15. In addition, results on process disturbance rejection can be found in our full paper [18].

Acknowledgment

Financial support for this work from the NSF (ITR), CTS-0325246, is gratefully acknowledged.

References

[1] A. Armaou and P. D. Christofides. Plasma-enhanced chemical vapor deposition: Modeling and control. *Chem. Eng. Sci.*, 54:3305–3314, 1999.

[2] A. Armaou, C. I. Siettos, and I. G. Kevrekidis. Time-steppers and 'coarse' control of distributed microscopic processes. *Int. J. Robust Nonlin. Control*, 14:89–111, 2004.

[3] K. J. Åström. *Introduction to Stochastic Control Theory*. Academic Press, New York, 1970.

[4] P. D. Christofides. *Nonlinear and Robust Control of Partial Differential Equation Systems: Methods and Applications to Transport-Reaction Processes*. Birkhäuser, Boston, 2001.

[5] S. F. Edwards and D. R. Wilkinson. The surface statistics of a granular aggregate. *Proc. R. Soc. Lond. A*, 381:17–31, 1982.

[6] K. A. Fichthorn and W. H. Weinberg. Theoretical foundations of dynamic Monte Carlo simulations. *J. Chem. Phys.*, 95:1090–1096, 1991.

[7] M. A. Gallivan and R. M. Murray. Reduction and identification methods for Markovian control systems, with application to thin film deposition. *Int. J. Robust Nonlin. Control*, 14:113–132, 2004.

[8] P. E. Gill, W. Murray, M. A. Saunders, and M. H. Wright. Procedures for optimization problems with a mixture of bounds and general linear constraints. *ACM Trans. Math. Software*, 10:282–298, 1984.

[9] D. T. Gillespie. A general method for numerical simulating the stochastic time evolution of coupled chemical reactions. *J. Comp. Phys.*, 22:403–434, 1976.

[10] M. A. Katsoulakis, A. J. Majda, and D. G. Vlachos. Coarse-grained stochastic processes and Monte Carlo simulations in lattice systems. *J. Comp. Phys.*, 186:250–278, 2003.

[11] K. B. Lauritsen, R. Cuerno, and H. A. Makse. Noisy Kuramote-Sivashinsky equation for an erosion model. *Phys. Rev. E*, 54:3577–3580, 2003.

[12] Y. Lou and P. D. Christofides. Estimation and control of surface roughness in thin film growth using kinetic Monte-Carlo models. *Chem. Eng. Sci.*, 58:3115–3129, 2003.

[13] Y. Lou and P. D. Christofides. Feedback control of growth rate and surface roughness in thin film growth. *A.I.Ch.E J.*, 49:2099–2113, 2003.

[14] Y. Lou and P. D. Christofides. Feedback control of surface roughness of GaAs (001) thin films using kinetic Monte-Carlo models. *Comp. & Chem. Eng.*, 29:225–241, 2004.

[15] Y. Lou and P. D. Christofides. Feedback control of surface roughness in sputtering processes using the stochastic Kuramoto-Sivashinsky equation. *Comp. Chem. Eng.*, 29:741–759, 2005.

[16] Y. Lou and P. D. Christofides. Feedback control of surface roughness using stochastic PDEs. *AIChE J.*, 51:345–352, 2005.

[17] M. Marsili, A. Maritan, F. Toigo, and J.R. Banavar. Stochastic growth equations and reparametrization invariance. *Rev. Mod. Phys.*, 68:963–983, 1996.

[18] D. Ni and P. D. Christofides. Construction of stochastic PDEs for feedback control of surface roughness in thin film deposition. *Int. J. Robust. Nonlin. Control,* submitted.

[19] D. Ni and P. D. Christofides. Dynamics and control of thin film surface microstructure in a complex deposition process. *Chem. Eng. Sci.*, 60:1603–1617, 2005.

[20] D. Ni and P. D. Christofides. Multivariable predictive control of thin film deposition using a stochastic PDE model. *Ind. Eng. Chem. Res.,* to appear, 2005.

[21] D. Ni, Y. Lou, P. D. Christofides, L. Sha, S. Lao, and J. P. Chang. Real-time carbon content control for PECVD ZrO_2 thin film growth. *IEEE Trans. Semiconduct. Manufact.*, 17:221–230, 2004.

[22] S. Park, D. Kim, and J. Park. Derivation of continuum stochastic equations for discrete growth models. *Phys. Rev. E*, 65:015102(R), 2002.

[23] C. I. Siettos, A. Armaou, A. G. Makeev, and I. G. Kevrekidis. Microscopic/stochastic timesteppers and "coarse" control: a KMC example. *AIChE J.*, 49:1922–1926, 2003.

[24] M. E. Taylor and H. A. Atwater. Monte Carlo simulations of epitaxial growth: comparison of pulsed laser deposition and molecular beam epitaxy. *Appl. Surf. Sci.*, 127:159–163, 1998.

[25] A. Theodoropoulou, R. A. Adomaitis, and E. Zafiriou. Inverse model based real-time control for temperature uniformity of RTCVD. *IEEE Trans. Semiconduct. Manufact.*, 12:87, 1999.

[26] D. G. Vlachos. Multiscale integration hybrid algorithms for homogeneous-heterogeneous reactors. *AIChE J.*, 43:3031, 1997.

[27] D. D. Vvedensky. Edwards-Wilkinson equation from lattice transition rules. *Phys. Rev. E*, 67:025102(R), 2003.

[28] D. D. Vvedensky, A. Zangwill, C. N. Luse, and M. R. Wilby. Stochastic equations of motion for epitaxial growth. *Phys. Rev. E*, 48:852–862, 1993.